

Experimental and theoretical comparison between absorption, total electron yield, and fluorescence spectra of rare-earth M_5 edges

M. Pompa, A. M. Flank, and P. Lagarde

Laboratoire pour l'Utilisation du Rayonnement Electromagnetique, Bâtiment 209d, Centre Universitaire, 91405 Orsay, France

J. C. Rife

Naval Research Laboratory code 6686, 4555 Overlook Avenue Southwest, Washington, D.C. 20375

I. Stekhin

Physical Department, Rostov State University, Rostov-on-Don 344104, Russia

M. Nakazawa, H. Ogasawara, and A. Kotani

Institute for Solid State Physics, University of Tokyo, Roppongi, Minato-ku, Tokyo 106, Japan

(Received 26 December 1996)

Besides the now well-known self-absorption effect, several phenomena related to the multiplet structure of the intermediate state may occur which render x-ray fluorescence different from the true absorption in $3d$ transition metals at the L edge and at the $M_{4,5}$ edges of rare earths. Special selection rules of the radiative de-excitation process play an important role there. We have measured the absorption coefficient of thin films of lanthanum, samarium, and thulium deposited on an aluminum foil, at room temperature, through the simultaneous detection of the transmission, total electron yield, and 150-eV bandwidth fluorescence yield. The latter result shows differences as compared to the other two, and exhibits polarization effects depending upon the angle between incident and outgoing photons. The resonant x-ray fluorescence spectrum is calculated using an atomic model, and then integrated over the emitted energy, to predict the fluorescence yield spectrum. Very good agreement is obtained between the theory and experiment. [S0163-1829(97)09528-3]

INTRODUCTION

Fluorescence yield (FY) measurements of core-level absorption edge spectra have a variety of advantages over total-electron-yield (TEY) measurements including bulk sampling depth, low background, and insensitivity to applied electric and magnetic fields. In the case of FY from occupied valence states, the escape depth of the lower-energy emission is greater than the penetration depth of the incident radiation, so that absorption spectra contrast can be greatly reduced. This saturation is usually encountered only in grazing incidence in TEY from very thin samples (of the order of 1 nm), because of the small escape depths of 0.5–2 nm of the secondary or low-energy Auger electrons measured (with contributions from farther ranging higher energy Auger electrons in TEY).¹ For case of FY from transition metals and rare earths with partially filled, localized $3d$ and $4f$ orbitals having sharp, intense multiplet spectra, the emission from each state is resonance fluorescence. In that situation, self-absorption of the emission distorts the spectrum, reducing the relative magnitude of the largest absorption features as in saturation. Self-absorption and saturation can limit FY to the study of dilute elements in absorbing matrices or thin films.

However, FY spectra can differ from true absorption not only due to the escape versus penetration depth dependence and self-absorption, but also due to relaxation processes of the intermediate state. More fundamentally, the Auger and fluorescent decay rate can vary across a multiplet, leading to a FY absorption spectrum that is a product of the emission rate and the absorption, so long as the interference effect is

disregarded.² Synchrotron radiation studies have also shown a variety of resonant effects on fluorescence spectra (and Auger), since emission and absorption are coupled due to the short lifetimes. For localized, core-level excitonic states in insulators, valence-band emission is lowered in energy due to screening by the core exciton.³ For delocalized valence- and conduction-band states, momentum is conserved, leading to emission from the same point in the Brillouin zone.⁴ Ma, in particular, considered the FY as resonant inelastic scattering and cautioned that FY may represent a partial cross section.⁵ In the last few years, these effects have been shown experimentally through their consequences on x-ray magnetic dichroism, which changes depending on the energy of the fluorescence line which is monitored.^{6,7} A theoretical approach to the problem has been presented recently, where the limit of the polarization dependence for magnetic studies has been analyzed.⁸

This work is part of a larger study of the magnetic nature of small clusters of rare earths in rare-gas matrices.⁹ Here we have chosen to examine transmission, TEY, and FY of a thin film to minimize spectral distortions due to saturation and self-absorption. The experiments show that the FY is distinctly different from the transmission and TEY, with one of the three major transitions missing in the case of Tm, for instance, and that these differences from TEY are fitted well by resonant inelastic scattering calculations using an atomic model. Moreover these calculations predict the dependence of the FY with the angle between the incident and the fluorescence photons, in particular in the case of Sm and La.

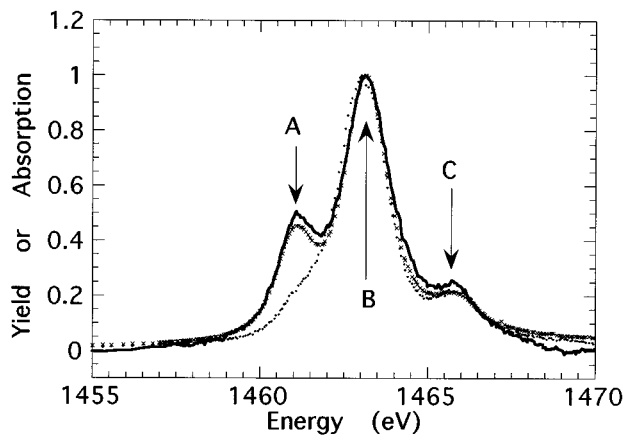


FIG. 1. Comparison between the transmission (solid line), the total electron yield (crosses), and the fluorescence yield (dots) results of a thin film of thulium at the M_5 edge.

I. EXPERIMENT

We simultaneously measured the transmission, TEY, and FY of thin films of La, Tm, and Sm at the M_5 edges for several incidence angles. The measurements were made at beamline SA-32 of the Super-ACO storage ring at LURE. The monochromator was a scanning two-crystal (1, -1) type with beryl crystals and delivered radiation with a bandpass of about 0.5 eV in the range of the Tm $M_{4,5}$ edges. The energy calibration is within 0.05 eV. The incident beam intensity was measured by a thin-film TEY monitor. Beryllium filters just upstream of the monochromator, and an UHV experimental chamber, were used to block low-energy light. The monochromatized radiation was greater than 99% linearly polarized in the horizontal. The focused spot on sample was about 500 μm horizontally and 300 μm vertically in normal incidence. The thin-film sample was mounted with its normal in the horizontal on a rotary motion with rotation around the vertical (angular accuracy of about 3°). FY was measured by a seven-element Ge detector (Eurisyss-Mesures), with an energy resolution of typically 150 eV. The whole detector was set successively at 90° and 45° of the incident photon direction. Three diodes of this seven-element array being in the plane of incidence, we could simultaneously measure three fluorescence signals at different angles between the incident photon beam and the outgoing one. TEY was measured by monitoring the drain current of the sample, while transmission was measured by current generated in a 1-cm² silicon photodiode located behind the sample.

The rare-earth films were deposited by evaporation in a vacuum of a few 10^{-9} Torr at room temperature on an unsupported Al film 700 nm thick. Evaporation rate was less than 0.1 nm/min. The film thickness was measured with a quartz-crystal thickness monitor. Given the vacuum and high gettering of La, Tm, or Sm, it is likely that the films were almost entirely oxidized.

II. RESULTS AND INTERPRETATION

Figure 1 shows Tm M_5 absorption derived from transmission, TEY, and FY of the Tm thin film measured simultaneously at an incidence angle (relative to the sample normal) of 64°. The FY spectrum is the sum of signals collected by

the seven elements with the detector set at 90° from the incident light. An incidence angle close of 64° was chosen in order to obtain counting rates for each of the detectors that are approximately equal. By summing over all detectors, we improve the signal-to-noise ratio without any loss of information since it can be proved (see below) that the collection angle is not important in this case of thulium. The spectra had flat backgrounds subtracted, and have been normalized to one at the most intense peak. The TEY absorption spectrum in Fig. 1 is not saturated and, surprisingly, shows a slightly greater magnitude absorption than the transmission results. This could be due to the relative values of the sampling depth of the TEY, the photon absorption length, and the sample thickness. However, the film was only 5 nm thick, the Tm escape depth was calculated in the range 6.5–11.5 nm, and the absorption length was 13 nm,¹⁰ while our transmission yields an absorption length of 34 nm. Such a difference has been already reported in thin Ce films.¹¹ Moreover the film could be laterally inhomogeneous and the transmission “saturated.” Islands, for example, covering 0.2 of the surface could reduce the relative-transmission-derived absorption of the most intense peak approximately as observed.

The spectra collected by TEY or transmission have the same features as previous Tm³⁺ $M_{4,5}$ absorption edge observations^{10,12–15} and calculations.^{10,12,16} The three peaks at 1461.1, 1463.1, and 1465.7 eV are transitions from the $3d^{10}4f^{12} \ ^3H_6$ ground state to the $3d^94f^{13}$ excited states, which correspond mainly to 3H_6 , 3G_5 , and 1H_5 , respectively. Because the 4f orbitals are well localized, the trivalent absorption features are very similar in materials such as Tm₂O₃, bulk Tm, and TmAl₂. Differences of up to 30% in the relative magnitudes of TEY peaks are observed for different compounds,¹³ but the differences could depend on surface preparation. A distinctly different, divalent Tm absorption spectrum with a single peak is observed at about 1460 eV (on our scale) for single atoms, clusters of less than 13 atoms, clean but rough surfaces, and some compounds such as TmTe.¹⁵ In Fig. 1, the differences between the FY and the two other measurements are obvious, with the lower-energy peak almost missing in FY.

As perhaps the best representative of the absorption, we have fitted the TEY data of Fig. 1 with Voigt functions. The best fit is with a Lorentzian full width at half maximum (FWHM) of 0.98 eV for the $\Delta J=0$ lower-energy peak, and 1.6 eV for the two $\Delta J=-1$ higher-energy peaks and with a Gaussian FWHM broadening of 0.54 eV for all peaks. The Gaussian broadening extracted is in reasonable agreement with resolution of our beryl crystal monochromator. The natural lifetime Lorentzian broadening compares with the calculation of Thole *et al.*, who assumed a Lorentzian FWHM of 0.8 eV (and a Gaussian broadening of 0.94-eV FWHM).¹⁰ Because of the uncertainties about the exact thicknesses of the sample, we did not try to extract the true absorption coefficients from our measurements, as was previously done.¹⁰

Figure 2 compares the three corresponding spectra on a thin film of samarium. In that case, because we will see that the fluorescence is angle dependent, only the FY data taken from the single detector located at 90° from the incident photon beam have been plotted. The remarks which have

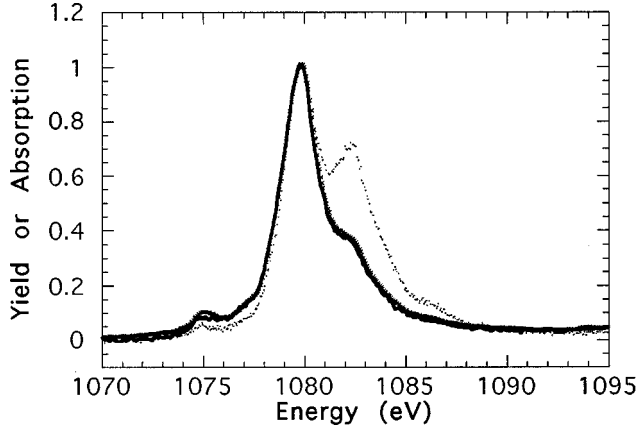


FIG. 2. Comparison between the transmission (solid line) the total electron yield (crosses) and the fluorescence yield (dots) results of a thin film of samarium at the M_5 edges.

been made for Tm are also applied in this case, with essentially the TEY and absorption spectra identical, while the FY exhibits marked differences from the two other experiments.

A. Interpretation

In the case of Tm, the primary difference in our spectra is the missing $\Delta J=0$ FY peak. Of course we have at first tried to explain the differences by a self-absorption effect which could affect the low-energy component. This implies a non-physical energy shift of the fluorescence line, compared to the absorption, which allows us to rule out this explanation. Another possibility is a linear dichroism in the resonant fluorescence from Tm_2O_3 polycrystals, which is observed with Zeeman splitting in rare earths.¹⁶ This requires high magnetic fields and low temperatures for sufficient Zeeman splitting in the rare earths. Linear dichroism has been observed in TEY at room temperature for a submonolayer of Dy on various substrates, and attributed to intense interfacial electric fields.^{17,18} It is difficult to see how a strong enough field exists in our thicker polycrystalline Tm_2O_3 layers. The crystal-field splitting in bulk Tm_2O_3 itself, while significant, is not large enough to leave only the ground state substantially populated (the first three excited states are 4, 11, and 27 meV above the ground state¹⁹).

The calculations of the $3d$ core x-ray-absorption spectrum (XAS) and the resonant x-ray fluorescence spectra (RXFS) are made by a free-ion model^{20,21} with, for instance in the case of thulium, a $4f^{12}$ configuration. The multiplet coupling effect originating from the Coulomb and exchange interactions and the spin-orbit interaction is fully taken into account using Cowan's program. The XAS is calculated in the form

$$F_{\text{XAS}}(\Omega) = \sum_i | \langle i | T | g \rangle |^2 \frac{\Gamma}{(\Omega + E_g - E_i)^2 + \Gamma^2}, \quad (1)$$

where $|g\rangle$ is the Hund's rule ground state 3H_6 (with energy E_g), $|i\rangle$ represents each final state (with energy E_i) which is excited by the optical dipole transition operator T between $3d$ and $4f$ states, Ω is the incident photon energy, and Γ represents the $3d$ core-hole lifetime broadening. Using the formula of the coherent second-order optical process, the spectrum of the $4f \rightarrow 3d$ RXFS is given by

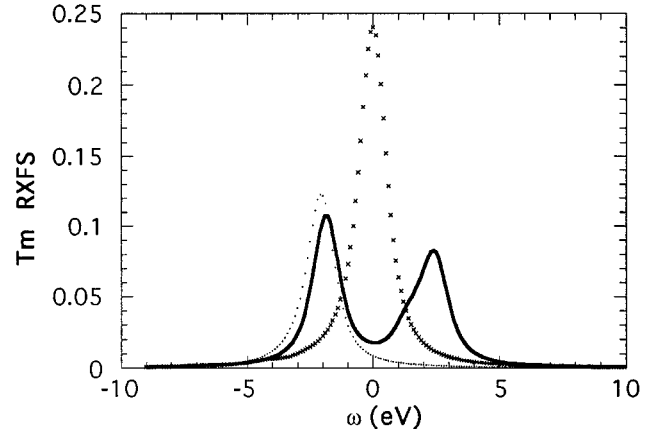


FIG. 3. Resonant x-ray fluorescence scattering (RXFS) of Tm for three different incident energies labelled in Fig. 1: dots, energy of peak A; crosses, energy of peak B (the amplitude has been divided by 5); solid line, energy of peak C, showing the inelastic contribution. ω is the emitted photon energy, as defined in Eq. (3).

$$F_{\text{RXFS}}(\Omega, \omega) = \sum_f \left| \sum_i \frac{\langle f | T | i \rangle \langle i | T | g \rangle}{E_i - E_g - \Omega - i\Gamma} \right|^2 \times \delta(E_g + \Omega - E_f - \omega), \quad (2)$$

where $|i\rangle$ and $|f\rangle$ are intermediate and final states with energies E_i and E_f , respectively, and ω is the emitted photon energy. It is to be noted that the intermediate state $|i\rangle$ is the same as the final state of the $3d$ XAS. Figure 3 shows the RXFS of Tm as a function of the outgoing energy ω for selected incident photon energies Ω within an energy scale where the zero corresponds to the energy of the main absorption line (labeled B in Fig. 1). In this figure, only three incident energies have been considered, which corresponds respectively to the energy positions of the three peaks A, B, and C in the absorption spectrum of thulium. The spectrum of FY is then obtained by integrating $F_{\text{RXFS}}(\Omega, \omega)$ over the emitted photon energy ω :

$$F_{\text{FY}}(\Omega) = \int F_{\text{RXFS}}(\Omega, \omega) d\omega. \quad (3)$$

If we take into account that the polarization vector of the incoming photon is in the scattering plane, and denote the angle between the incoming and fluorescence photon directions as Θ , then Eq. (3) is written as

$$F_{\text{FY}}(\Omega) = \sum_q \sum_f \left| \sum_i \frac{\langle f | C_q^{(i)} | i \rangle \langle i | C_0^{(i)} | g \rangle}{E_i - E_g - \Omega - i\Gamma} \right|^2 A_q(\Theta), \quad (4)$$

where $A_q(\Theta) = \frac{1}{2}(1 + \sin^2 \Theta)$ for $q=1$ and -1 , and $\cos^2 \Theta$ for $q=0$, and C_q is the normalized spherical harmonic representing the dipole transition. Here is to be noted that the $3d$ core hole lifetime broadening Γ in Eqs. (1), (2), and (4) is dominated by the Auger decay, and the radiative decay is negligibly smaller than the Auger one. This is an important point in studying the difference between FY and XAS. If the radiative decay was the dominant channel in Γ , any variation in the radiative decay strength would be unimportant for FY, as found from Eq. (4).

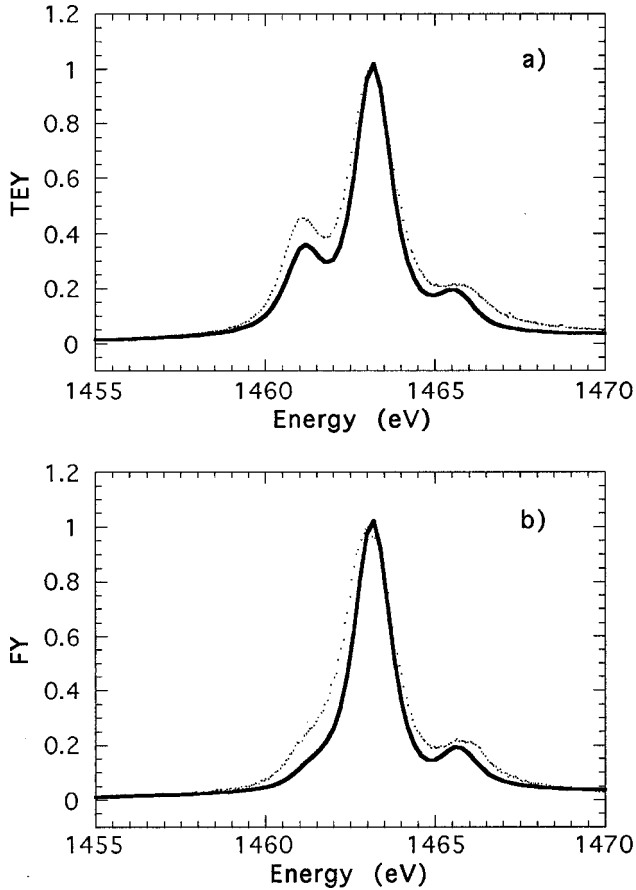


FIG. 4. Comparison between experiment (dots) and theory (solid line) for the absorption coefficient (a) measured by TEY, and for the fluorescence yield (b) of Tm.

The calculated results of XAS and FY are shown in Fig. 4 in the case of thulium. The value of Γ is taken to be 0.5 eV, and then the obtained spectra F_{XAS} and F_{FY} are convoluted by a Gaussian function with width 0.6 eV (FWHM). The XAS exhibits three peaks A, B, and C. Peak A corresponds to the excited state 3H_6 , and peak B corresponds mainly to 3G_5 (including 20% of 3H_5), while peak C consists of 1H_5 (54%), 3H_5 (37%), and 3G_5 (9%). The intensities of XAS and FY are taken so that their maximum values coincide each other. The calculated FY shows features B and C very similar to those of XAS, whereas peak A is almost missing in FY.

In order to find the origin of the missing peak A in FY, we take a look to the calculated RXFS as a function of ω for various values of Ω shown in Fig. 3. It is found that for Ω corresponding to A and B we have almost a single peak in F_{RXFS} , whose final state is the same as the ground state term 3H_6 . Therefore, these RXFS corresponds to the elastic resonant x-ray scattering. However, for Ω corresponding to C, we find an inelastic scattering peak in addition to the elastic one. The final state of this inelastic peak corresponds mainly to the 1I_6 final state, which is obtained by the spin-flip excitation from the ground state 3H_6 . The reason why we have a strong inelastic scattering intensity for the XAS peak C is that the intermediate state C is a strong mixture between 1H_5 and 3H_5 states, and then the 1H_5 component can decay radiatively to the final state 1I_6 , while the 3H_5 component decays to the 3H_6 final state.

If we take into account only the elastic-scattering component, the FY has a single peak B with a weak shoulder at the positions A and C, because $F_{\text{FY}}(\Omega)$ is then roughly given by $[F_{\text{XAS}}(\Omega)]^2$. In effect if we confine ourselves into the elastic scattering ($|f\rangle=|g\rangle$) and fix a specific state $|i\rangle$ with $\Omega=E_i-E_g$, then Eq. (1) gives $F_{\text{XAS}}=|\langle i|T|g\rangle|^2/\Gamma$, and Eqs. (2) and (3) give $F_{\text{FY}}=|\langle i|T|g\rangle|^4/\Gamma^2$, from which we obtain $F_{\text{FY}}=F_{\text{XAS}}^2$. Then we add to this FY the inelastic component which increases the spectral weight at the position of peak C, and finally we find that FY behaves similarly to XAS for B and C, while peak A is almost missing.

B. Polarization effects

The formalism described above allows us to predict the dependence of the FY as a function of the angle Θ between the incoming photon and the fluorescence one. In order to do these experiments, the seven-element detector has been set successively with its central element at 90° and 45° , and the experiments have been performed on lanthanum and samarium where the polarization effects are expected to be stronger than for thulium, for which these calculations do not show such a dependence.

For one position of the detector, the measured intensity from each of the three detectors situated in the incidence plane has been scaled by a factor which takes into account the solid angle seen by each diode. Moreover, in going from one detector angle (45°) to the other one (90°), the best signal-to-noise ratio is obtained for a different angle of incidence of the photon on the sample, assumed of course to be polycrystalline. Therefore, we have set the detector in such a way that, for the two positions, one detector corresponds to the same angle Θ . In that case, the two sets of measurements can be normalized since two data relate to the same Θ . We then have altogether four different angles Θ of about 25° , 45° , 60° and 90° , with an average accuracy of $\pm 5^\circ$ which corresponds to the diameter of each diode. It could be thought that this normalization method could be cross checked by using the TEY signal which is not expected to exhibit any polarization effect, and then by using the formula of the fluorescence yield as a function of the geometrical setup (incidence and taking off angles). Actually, because

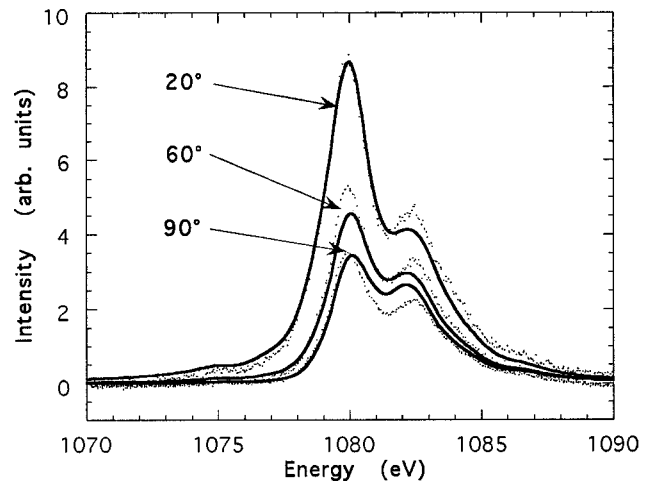


FIG. 5. Experimental (dots) and theoretical (solid lines) fluorescence spectra of samarium at different detection angles.

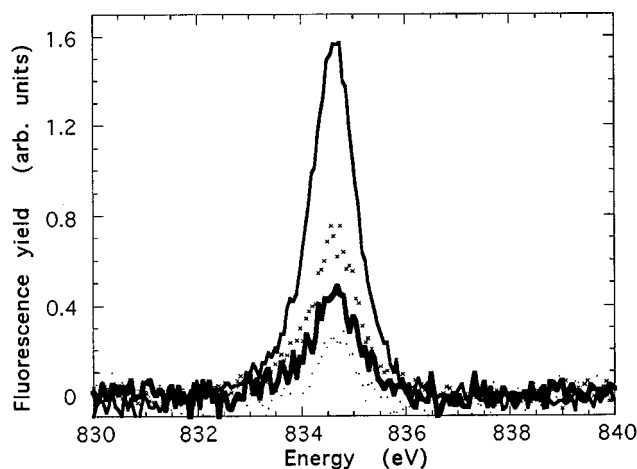


FIG. 6. La M_5 fluorescence yield as a function of the detection angle. Solid line, 20° ; crosses, 45° ; thick solid line, 60° ; dots, 70° .

the thickness of the sample is smaller than the photon or the photoelectron mean free paths, any inhomogeneity on the sample thickness will introduce large errors when attempting to quantify the effect of the change of the angle of incidence.

Figure 5 compares experiments and calculations for the M_5 FY of samarium. A scaling factor between theory and experiment has been obtained for one angle, and then applied to the other angles. This figure shows that the theoretical model is fully able to predict, as for thulium, the shape of the FY but also its polarization dependence. In the case of La, the ground state is a singlet state with $4f^0$ configuration, so that the M_5 FY is a single peak whose angular dependence is simple. The summation over q then reduces to a single term with $q=0$, and the FY is proportional to $\cos^2 \Theta$. Figure 6 shows the M_5 edge of lanthanum as a function of the angle Θ , while Fig. 7 compares the intensity of this line with a theoretical $\cos^2 \Theta$ function. The point corresponding to an angle of 90° does not fit well with the theoretical curve, but in that case the counting rate is very low, and therefore the error in the intensity very large (actually this curve has not been reported in Fig. 6). The overall agreement between the theory and the measured values is nevertheless very satisfactory.

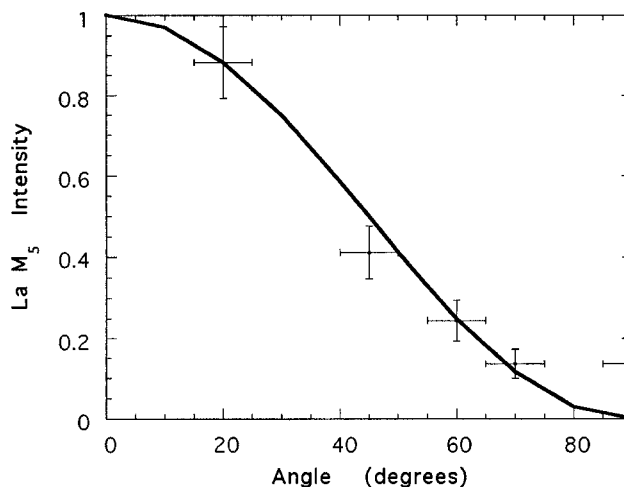


FIG. 7. Variation of the intensity of the M_5 line of lanthanum as a function of the angle Θ between the incident and the fluorescence photons. The solid line is a $\cos^2 \Theta$ function.

CONCLUSION

We have shown in this paper that, for quasiautomatic transitions such as the $M_{4,5}$ edges of rare earths, special selection rules for the radiative decay (fluorescence) may render the fluorescence yield distinctly different from the total electron yield or the absorption cross section. This effect comes from an inelastic decay channel which opens up for selected absorption transitions, and increases the radiative deexcitation probability compared to the elastic case. The experimental results obtained in the cases of La, Sm, and Tm have been quantitatively explained within an atomic model which first calculates the resonant x-ray fluorescence spectrum. The differences between fluorescence yield and true absorption results question the applicability of the method to problems involving rare earths like x-ray magnetic dichroism, where FY has the advantage, compared to the total electron yield, to be insensitive to magnetic fields. Moreover the fluorescence yield exhibits a polarization dependence with the angle between the incident and fluorescence photons which has also been modeled using the same formalism. In that sense, these results have to be related to previously published data,⁶⁻⁸ which dealt mostly with x-ray magnetic circular dichroism (XMCD) experiments.

¹A. Erbil, G. S. Cargill III, R. Frahm, and R. F. Boehme, Phys. Rev. B **37**, 2450 (1988).

²F. M. F. de Groot, M. A. Arrio, Ph. Saintavit, Ch. Cartier, and C. T. Chen, Solid State Commun. **92**, 991 (1994).

³W. L. O'Brien, J. Jia, Q.-Y. Dong, T. A. Callcott, K. E. Miyano, D. L. Ederer, D. R. Mueller, and C.-C. Kao, Phys. Rev. Lett. **70**, 238 (1993).

⁴P. Johnson and Y. Ma, Phys. Rev. B **49**, 5024 (1994).

⁵Y. Ma, Phys. Rev. B **49**, 5799 (1994).

⁶L.-C. Duda, J. Stöhr, D. C. Mancini, A. Nilsson, N. Wassdahl, J. Nordgren, and M. G. Samant, Phys. Rev. B **50**, 16 758 (1994).

⁷C. F. Hague, J.-M. Mariot, G. Y. Guo, K. Hricovini, and G. Krill, Phys. Rev. B **51**, 1370 (1995).

⁸M. van Veenendaal, J. B. Goedkoop, and B. T. Thole, Phys. Rev. Lett. **77**, 1508 (1996).

⁹A. M. Flank, P. Lagarde, R. Delaunay, M. Pompa, and C. Teodorescu, Physica B **208&209**, 773 (1995).

¹⁰B. T. Thole, G. Van der Laan, J. C. Fuggle, G. A. Sawatzky, R. C. Karnatak, and J.-M. Esteve, Phys. Rev. B **32**, 5107 (1985).

¹¹S. Turchini, R. Delaunay, P. Lagarde, J. Vogel, and M. Sacchi, J. Electron Spectrosc. Relat. Phenom. **71**, 31 (1995).

¹²G. Kaindl, W. D. Brewer, G. Kalkowski, and F. Holtzberg, Phys. Rev. Lett. **51**, 2056 (1983).

¹³G. Kaindl, G. Kalkowski, W. D. Brewer, B. Perscheid, and F. Holtzberg, J. Appl. Phys. **55**, 1910 (1984).

¹⁴A. Belhmi-Belhassan, R. C. Karnatak, N. Spector, and C. Bon-

- nelle, Phys. Lett. A **82**, 174 (1981).
- ¹⁵C. Blancard, J. M. Esteva, R. C. Karnatak, J. P. Connerade, U. Kuetsgens, and J. Holmes, J. Phys. B **22**, L575 (1989).
- ¹⁶J. B. Goedkoop, B. T. Thole, G. Van der Laan, G. A. Sawatzky, F. M. F. de Groot, and J. C. Fuggle, Phys. Rev. B **37**, 2086 (1988).
- ¹⁷M. Sacchi, O. Sakho, and G. Rossi, Phys. Rev. B **43**, 1276 (1991).
- ¹⁸M. Sacchi, O. Sakho, F. Sirotti, and G. Rossi, Appl. Surf. Sci. **56/58**, 1 (1992).
- ¹⁹J. B. Gruber, W. F. Krupke, and J. M. Poindexter, J. Chem. Phys. **41**, 3363 (1964).
- ²⁰S. Tanaka, K. Okada, and A. Kotani, J. Phys. Soc. Jpn. **62**, 464 (1993).
- ²¹A. Kotani (unpublished).